Ain Shams Engineering Journal (2015) 6, 803–817

Ain Shams University

Ain Shams Engineering Journal

www.elsevier.com/locate/asej
www.sciencedirect.com

ELECTRICAL ENGINEERING

# Analysis and effect of multi-fuel and practical constraints on economic load dispatch in the presence of Unified Power Flow Controller using UDTPSO

**Chintalapudi V. Suresh** *, **Sirigiri Sivanagaraju**

*EEE Department, UCEK, JNTUK, Kakinada, AP 533003, India*

Received 2 September 2014; revised 6 December 2014; accepted 23 December 2014
Available online 7 February 2015

**KEYWORDS**

Multi-fuel cost;
Ramp-rate limits;
Prohibited operating zones;
UPFC;
Optimal location;
UDTPSO

**Abstract** This paper presents an attempt to analyze the effect of multi-fuel and practical constraints on economic load dispatch problem using a novel uniform distributed two-stage particle swarm optimization (UDTPSO) algorithm without and with unified power flow controller (UPFC) while satisfying equality, inequality, practical constraints such as ramp-rate and prohibited operating zone (POZ) limits and device operating limits. A Novel severity function is formulated based on the transmission line overloads and bus voltage violations to identify an optimal location to install UPFC. A multi-objective optimization problem is solved for multi-fuel non-convex cost and transmission power loss objectives. Obtained results for considered standard test functions and electrical systems indicate the effectiveness of the proposed algorithm and can obtain efficient solution when compared to existing methods. Hence, the proposed method is a promising method and can be easily applied to optimize the power system objectives.


## 1. Introduction

Economic dispatch (ED) is one of the most challenging tasks in power system analysis. The objective of this task was to maximize the utilization of lowest cost of generation while satisfying physical and operating constrains. Nowadays, the degradation of fuel levels and the increased cost of fossil fuels such as, coal, oil, and natural gas for power generation turn our interest toward ED problem. Generally power plants are equipped with multiple steam valve turbines; hence, the valve loading effect should be considered in ED problem. In this paper, more realistic problem is by stating that, power plants are supplied by multiple fuels and the effect of this should also be considered in ED problem.

Conventionally, Interior point methods, many mathematical programming approaches, Gradient based optimization algorithms, Nonlinear Programming (NLP), Linear Programming (LP) methods and Newton method have been applied for

* Corresponding author.
E-mail address: venkatasuresh3@gmail.com (C.V. Suresh).
Peer review under responsibility of Ain Shams University.

Production and hosting by Elsevier

http://dx.doi.org/10.1016/j.asej.2014.12.011

economic dispatch problem [1,2]. These methods have several limitations in handling non-linear, discrete–continuous functions while satisfying constraints [3] and these methods are facing some difficulties in handling the objectives having multiple local minima. To overcome these limitations of classical optimization algorithms, recently various heuristic optimization algorithms have been developed such as Genetic Algorithm (GA) [4,5], Simulated Annealing (SA) [6,7], Tabu Search (TS) [8], Differential Evolution (DE) [9–11], Harmony Search (HS) [12], biogeography based optimization (BBO) [13,14], Evolutionary Programming (EP) [15,16], artificial immune system [17], quantum genetic algorithm [18], enhanced cross-entropy [19] and Particle Swarm Optimization (PSO) [20–23] methods have proved its effectiveness in solving economic load dispatch problems. These heuristic optimization algorithms often provide reasonable and fast solutions but do not guarantee in obtaining global best solution. GA suffers from the premature convergence; SA needs fine tuning of control parameters which degrades the system performance. The modifications in PSO algorithm were proposed by [24–29] and are applied for solving various optimization problems in electrical power engineering. The OPF problem was solved based on two stage initialization process [30] by avoiding mutation operation in DE algorithm. Because of this, the final convergence of the OPF problem is obtained in less time with enhanced accuracy.

Flexible AC Transmission System (FACTS) controllers are equipped with power semi-conductor converters; this enhances the capability of controlling various electrical parameters in transmission circuit. Some of the popular devices include, Thyristor controlled series compensator (TCSC), Static VAr compensator (SVC), Unified power flow controller (UPFC), etc. Modeling and incorporation of these devices in conventional power flow studies were presented in [31,32]. Out of these devices, TCSC can control the transmission line inductive reactance so as to control the active power flow. SVC can be used to absorb/inject the reactive power at a bus to control the voltage magnitude. UPFC can handle active and reactive power flows in transmission lines and voltage magnitude at buses simultaneously or any combination thereof, provided no operating and system limits are violated [33].

To obtain the better functionality of UPFC, it is necessary to identify proper installation location in a given system with appropriate device settings. One of the critical power system problems is blackout. To prevent this, the transmission line loadings and bus voltage magnitudes need to be considered to analyze the system security/severity. Recently, majority of research concentrates in finding an optimal location to install UPFC and various FACTS devices using evolutionary optimization techniques [34–37]. Optimal location of UPFC can be identified through contingency selections to enhance the steady state security level [38–42]. Differential Evolution algorithm has been successfully implemented to minimize generation fuel cost in the presence of FACTS devices such as TCSC and TCPS [43].

Generally power plants are equipped with multiple valves in order to get controlled output power. In real time power system operation, the effect of prohibited operating zones needs to be considered due to physical limitations and vibrations in the shaft bearings. The problem with all these constraints such as multi-fuel, ramp-rate and POZ limits turns the problem into more complicated one. Hence there is a need of more accurate optimization algorithm to solve the OPF problem. In this paper, a newly developed heuristic optimization algorithm based on uniform distribution of control variables to start the iterative process with good initial value and two stage initialization processes to reach final best value in less number of iterations are implemented along with the conventional PSO algorithm, called UDTPSO is proposed to solve OPF problem which is formulated as a nonlinear optimization problem while satisfying equality, inequality and practical constraints in a given power system. The objective functions formulated are quadratic cost, quadratic cost with valve loading effect, multi-fuel quadratic cost and multi-fuel non-convex cost functions. The effect of multi-fuel and practical constraints is analyzed in the presence of UPFC. The optimal location of UPFC is identified based on the transmission line overloads and bus voltage violations. The performance of the proposed methodology is tested on standard Himmelblau and sphere functions and electrical test systems such as IEEE-30 bus and Indian 62-bus systems. Obtained results demonstrate the effectiveness of the proposed method and are validated with the existing methods in the literature.

## 2. Problem formulation

Optimal Power Flow (OPF) problem optimizes the power system objectives, includes non-linear. In this paper, a newly developed heuristic optimization algorithm based on uniform distribution of control variables and two stage initialization processes are implemented along with the conventional PSO algorithm, called UDTPSO is proposed to solve OPF problem which is formulated as a nonlinear optimization problem while satisfying equality, inequality and practical constraints in a given power system. Finally a set of control variables are obtained as a solution for the problem while satisfying equality, inequality and practical constraints. Conventionally economic load dispatch problem includes generation fuel cost as an objective is optimized.

The problem can be formulated mathematically as a constrained nonlinear objective optimization problem as follows:

$$A = Min[J(x,u)] \tag{1}$$

Subjected to

$$g(x,u) = 0$$
$$h(x,u) \leqslant 0$$

where '$g$' and '$h$' are the equality and inequality constraints respectively and '$x$' is a control vector of dependent variables such as slack bus active power generation ($P_{g,slack}$), load bus voltage magnitudes ($V_L$) and generator reactive powers ($Q_G$) and vector '$u$' consists of control variables such as active powers ($P_G$) and voltages ($V_G$) of generators, transformer tap ratios ($T$) and shunt compensation ($Q_{Sh}$) and device control parameters.

### 2.1. Constraints

The above problem is optimized by satisfying the following equality, inequality, and practical constraints.

#### 2.1.1. Equality constraints

These constraints are typically load flow equations.

$$P_{Gk} - P_{Dm} - \sum_{m=1}^{NB} |V_k||V_m||Y_{km}|\cos(\theta_{km} - \delta_k + \delta_m) = 0 \quad (2)$$

$$Q_{Gk} - Q_{Dm} + \sum_{m=1}^{NB} |V_k||V_m||Y_{km}|\sin(\theta_{km} - \delta_k + \delta_m) = 0 \quad (3)$$

where '$P_{Gk}$, $P_{Dk}$' are the active and reactive power generations at $k$th bus, '$P_{Dm}$, $Q_{Dm}$' are the active and reactive power demands at $m$th bus, '$NB$' is number of buses, $|V_k|$, $|V_m|$ are the voltage magnitudes at $k$th and $m$th buses, '$\delta_k$, $\delta_m$' are the phase angles of voltages at $k$th and $m$th buses, $|Y_{km}|$, $\theta_{km}$ are the bus admittance magnitude and its angle between $k$th and $m$th buses.

### 2.1.2. In-equality constraints

$$\text{Generator bus voltage limits}: \quad V_{G_i}^{\min} \leqslant V_{G_i} \leqslant V_{G_i}^{\max}; \quad \forall i \in N_G \quad (4)$$

$$\text{Active Power Generation limits}: \quad P_{G_i}^{\min} \leqslant P_{G_i} \leqslant P_{G_i}^{\max}; \quad \forall i \in N_G \quad (5)$$

$$\text{Transformers tap setting limits}: \quad T_i^{\min} \leqslant T_i \leqslant T_i^{\max}; \quad i = 1, 2, \ldots, n_t \quad (6)$$

$$\text{Capacitor reactive power generation limits}: \quad Q_{Sh_i}^{\min} \leqslant Q_{Sh_i} \leqslant Q_{Sh_i}^{\max}; \quad i = 1, 2, \ldots, n_C \quad (7)$$

$$\text{Transmission line flow limit}: \quad S_{l_i} \leqslant S_{l_i}^{\max}; \quad i = 1, 2, \ldots, N_{line} \quad (8)$$

$$\text{Reactive Power Generation limits}: \quad Q_{G_i}^{\min} \leqslant Q_{G_i} \leqslant Q_{G_i}^{\max}; \quad \forall i \in N_G \quad (9)$$

$$\text{Bus voltage magnitude limits}: \quad V_i^{\min} \leqslant V_i \leqslant V_i^{\max}; \quad i = 1, 2, \ldots, N_{load} \quad (10)$$

where $n_t$ is the total number of taps, $n_C$ is the total number of VAr sources, $N_{load}$ is the total number load buses.

The abovementioned problem in Eq. (1) can be generalized using penalty factors as follows:

$$A_{m,aug}(x,u) = A_m(x,u) + R_1\left(P_{g,slack} - P_{g,slack}^{\lim}\right)^2 + R_2\sum_{i=1}^{N_{Load}}\left(V_i - V_i^{\lim}\right)^2 + R_3\sum_{i=1}^{N_G}\left(Q_{G_i} - Q_{G_i}^{\lim}\right)^2 + R_4\sum_{i=1}^{N_{line}}\left(S_{l_i} - S_{l_i}^{\max}\right)^2$$

where $R_1$, $R_2$, $R_3$ and $R_4$ are the penalty quotients having large positive value. The limit values are defined as

$$x^{\lim} = \begin{cases} x^{\max}, & x > x^{\max} \\ x^{\min}, & x < x^{\min} \end{cases}$$

Here '$x$' is the value of $P_{g,slack}$, $V_i$, $Q_{Gi}$.

### 2.1.3. Practical constraints

*2.1.3.1. Prohibited operating zones (POZs).* Because of the mechanical vibrations in shaft bearings, thermal stresses in the boilers, etc., synchronous generators at generating stations must avoid the operation in certain operating zones, popularly known as prohibited operating zones (POZs) to enhance the performance of the thermal units. This constraint can be incorporated in the problem formulation as

$$P_i = \begin{cases} P_i^{\min} \leqslant P_i \leqslant P_{i,1}^L \\ P_{i,k-1}^U \leqslant P_i \leqslant P_{i,k}^L \quad k = 2, 3, \ldots, n_i \\ P_{i,n_i}^U \leqslant P_i \leqslant P_i^{\max} \end{cases} \quad (11)$$

where $k$ is the index of prohibited zone of unit-$i$ and $n_i$ is the number of prohibited zones. $P_{i,k}^L$ and $P_{i,k}^U$ are the respective lower and upper limit of $k$th prohibited zone of $i$th generator.

*2.1.3.2. Ramp-rate limits.* Increasing/decreasing the power output of a generating unit follows ramp-rate limits, which is a function of resource size. The sudden change in load affects the generation output. This constraint can be modeled as

$$\max\left(P_{G_i}^{\min}, P_i^0 - DR_i\right) \leqslant P_{G_i} \leqslant \min\left(P_{G_i}^{\max}, P_i^0 + UR_i\right) \quad (12)$$

where, $P_i^0$ is the power generation of $i$th unit in previous hour. $DR_i$ and $UR_i$ are the respective decreasing and increasing ramp-rate limits of $i$th unit.

## 3. UPFC modeling

UPFC can be represented by two voltage sources representing fundamental components of output voltages of converter transformers. The equivalent circuit of UPFC power flow model and its respective power injection models are shown in Figs. 1 and 2. In this paper, the following rules are considered, to identify the proper device location so as to reduce the possible number of locations.

i. It should be located between two PQ buses and there should not be any shunt capacitors.
ii. It should not be placed in a line where tap changing transformer exists.

The complete mathematical modeling of the UPFC can be obtained by combining series connected and shunt connected voltage source models [44,45] and injecting respective powers at buses i and j. The power injection equations at respective buses including converter switching losses can be expressed as

$$P_{i,UPFC} = 0.02rb_{se}V_i^2\sin\gamma - 1.02rb_{se}V_iV_j\sin(\theta_i - \theta_j + \gamma) \quad (13)$$

$$P_{j,UPFC} = rb_{se}V_iV_j\sin(\theta_i - \theta_j + \gamma) \quad (14)$$

$$Q_{i,UPFC} = -rb_{se}V_i^2\cos\gamma \quad (15)$$

$$Q_{j,UPFC} = rb_{se}V_iV_j\cos(\theta_i - \theta_j + \gamma) \quad (16)$$

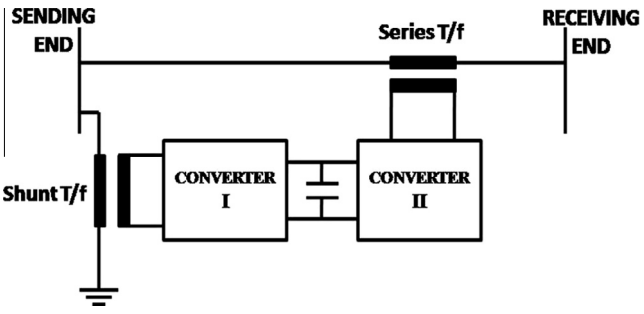


**Figure 1** Principle configuration of UPFC.

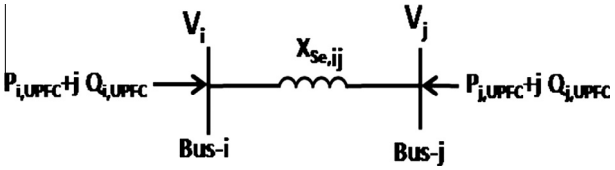


**Figure 2** Power injection model of UPFC.

The following limits are considered for the UPFC

$$0 < r < 0.1;\ 0 < \gamma < 360^{\circ};\ 0 < b_{se,ij} < 0.025$$

where '$r$' and '$\gamma$' are respective pu magnitude and phase angle of series voltage source converter of UPFC, operating within its specified limits. $V_i$, $V_j$ and $\theta_i$, $\theta_j$ are respective pu magnitude and angles at buses $i$ and $j$. '$X_{se,ij}$' and '$b_{se,ij}$' are the reactance and respective susceptance of series converter transformer. The complete incorporation and implementation procedure of UPFC in conventional NR-load flow described in [45] is followed in this work to analyze the effect of the same.

### 3.1. Optimal location

A severity function is formulated based on transmission line loadings and bus voltage magnitude violations under contingency conditions. The proposed severity function ($F_{severity}$) can be expressed as [46]

$$F_{Severity} = \sum_{i=1}^{N_{line}} \left( \frac{S_i}{S_i^{\max}} \right)^{2q} + \sum_{j=1}^{N_{bus}} \left( \frac{V_{j,ref} - V_j}{V_{j,ref}} \right)^{2r} \tag{17}$$

where $N_{line}$, $N_{bus}$ are the total number of lines and buses in a given system. $S_i$ and $S_i^{\max}$ are the present and maximum apparent powers of $i$th line. $V_{j,ref}$ and $V_j$ are the nominal voltage and present voltage values at $j$th bus. '$q$' and '$r$' are two coefficients used to penalize more or less overloads and voltage violations. These are considered to be equal to 2.

With this, the system security has been enhanced under contingency conditions by placing UPFC in a proper location. After performing contingency analysis, one of the highest critical lines is identified and also its corresponding total Number of Voltage Violation Buses (NVVB) and total Number of Over Loaded Lines (NOLL) are identified. After this the performance index is calculated by adding NOLL and NVVB for the respective contingencies. Now, remove this critical line from the system and identify the possible device installation locations for a given system. Place the UPFC in one of these locations and minimize the severity function. Repeat this process for all possible locations and identify the severity function values. Selecting the location which has the least severity function value in the presence of UPFC under contingency conditions is the best UPFC installation location. Finally system security has been enhanced with this location in the presence of UPFC.

## 4. Proposed UDTPSO

The performance of the existing Particle Swarm Optimization (PSO) is enhanced by implementing uniform distribution of problem control variables and two stage initialization processes. In this section, the complete methodology of the proposed method is explained.

### 4.1. Overview of existing PSO

The PSO is a population based selfadaptive stochastic optimization technique [26]. This algorithm starts with initialization of system control variables randomly as a population. These are treated as problem particles and each of one has its own position and velocity. In multi-dimensional solution search space, each of this particle moves toward optimal solution. Each particle adjusts its new velocity based on local and global best solutions. The updated position is calculated by adding new velocity with its earlier position. The new velocity and updated positions are calculated using the following expressions:

$$Vel_{ij}^{k+1} = W \times Vel_{ij}^{k} + C_1 \times rand_1 \times \left( Local_{ij}^{best} - X_{ij}^{k} \right) + C_2 \times rand_2 \times \left( Global_{i}^{best} - X_{ij}^{k} \right) \tag{18}$$

$$X_{ij}^{k+1} = X_{ij}^{k} + Vel_{ij}^{k+1} \tag{19}$$

where $X_{ij}^{k}$ and $Vel_{ij}^{k}$ are the present position and velocities of $i$th particle in $j$th dimension in $k$th iteration.

These new velocities and updated positions are calculated repeatedly for a pre-defined number of iterations reached. For minimization of the objective functions, the fitness function is evaluated using the following expression:

$$Fitness = \frac{1}{1 + A_{m,aug}}$$

The other important steps in the existing PSO method are initialization, iterations update, weight update, velocity update, position update, local best update, and global best update.

### 4.2. UDTPSO methodology

Many programming languages used for simulation of applications need to generate pseudo random numbers, which are effectively distributed using standard uniform distributions. Uniform distribution is one of the important members in the family of symmetric probability distribution. In this, all distributions have equal probability intervals. This is used to generate random variables between limits '$a$' and '$b$'. This distribution can be abbreviated as $U(a,b)$ [47].

#### 4.2.1. Initialization

Start the process by setting iteration is equal to zero. In this method, generate control variables uniformly rather than randomly as in existing PSO, between its minimum and maximum limits. In MATLAB environment, we have a flexibility to generate control variables using the following expressions:

Existing PSO: $a + (b - a) *$ rand (population number, particles number)
Proposed UDTPSO: random ('unif', a, b, population number, particles number)

While in other programming languages, the variables can be generated uniformly by following the uniform distribution procedure given in [48].

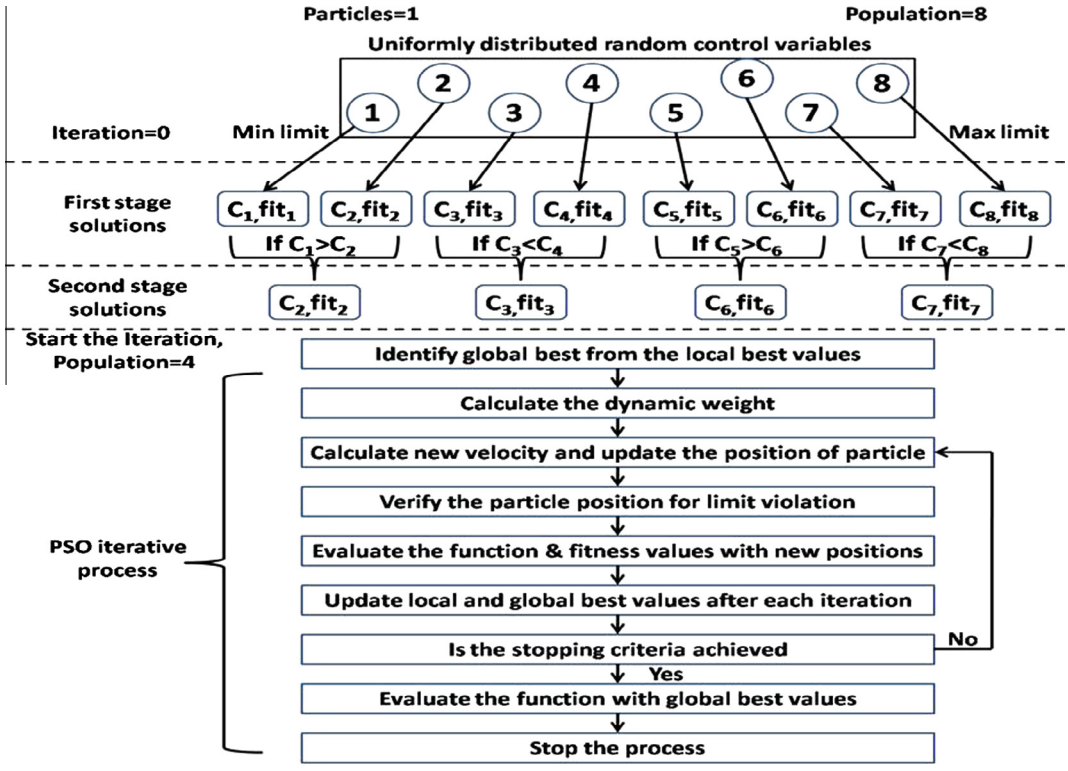


**Figure 3** Methodology of the proposed UDTPSO.

*4.2.2. Two stage initialization*

The first stage of the process is that, update the system data with newly generated control variables and evaluate the objective function and fitness values. The second stage of the process is that, obtaining the pairwise best population using comparison process between previously obtained solutions. The final solutions are treated as local best values. From these solutions, identify global best value. Start the iterative process by calculating dynamic weight and new velocities and update the position of the particles. The chaotic inertia weight [24,29] is calculated based on the experience of the previous positions and velocities of the particles. Because of this, the iterative process starts with large inertial weight to search global best values and decreases its value as iterations increase to benefit the local best values. Evaluate the function using new position of the particles and update global and local best values. The complete methodology is shown in Fig. 3.

## 5. Illustrative example

To test the effectiveness of proposed method a standard Himmelblau function given in Eq. (20) is used and the corresponding results are tabulated in Table 1. The comparison of convergence characteristics is shown in Fig. 4.

$$f(x_1, x_2) = \left(x_1^2 + x_2 - 11\right)^2 + \left(x_1 + x_2^2 - 7\right)^2 \tag{20}$$

It is observed from Fig. 4 that, the convergence of the proposed UDTPSO method starts with good function value and final best value is obtained within less number of iterations when compared to PSO. It is also observed that the computational time taken for the convergence is 1.1002 s which is 3.505 s less when compared with PSO.

Further the effectiveness of the proposed method is validated on the standard sphere function for 100 trails and the corresponding results are tabulated in Table 2. From this table, it is observed that, the standard deviation of the function values for 100 trails is almost zero, which means that the final best values have negligible deviation. The variation of the initial and final function values for 100 trails is shown in Fig. 5. From this figure, it is identified that, in majority of the trails, function final values are below their mean value. This is happened because of the effectiveness of the proposed algorithm.

## 6. Electrical system simulation results

In this section the proposed methodology is tested in standard IEEE-30 bus and Indian-62 bus electrical systems.

**Table 1** Comparison of optimal solution obtained for Himmelblau function.

| S. No | Parameters | Existing GA [49] | PSO | Proposed UDTPSO |
|---|---|---|---|---|
| 1 | $X_1$ | 3.003 | 2.996035929 | 3.000869494 |
| 2 | $X_2$ | 1.994 | 2.017203557 | 2.003608544 |
| 3 | Function value | 1.000e−03 | 0.004287118 | 0.000312504 |
| 4 | Computational time (s) | – | 4.6052 | 1.1002 |

### 6.1. Example-1

IEEE-30 bus system with 41 transmission lines is considered [8,50,51]. The total control variables in this system are 18, which include 6 active power generations and respective voltage levels, 4 tap settings of tap-changing transformers and 2 shunt VAr sources. The generator fuel cost function '$J$' is formulated as follows:

$$J = \sum_{i=1}^{N_G} FC_i \quad \$/h \tag{21}$$

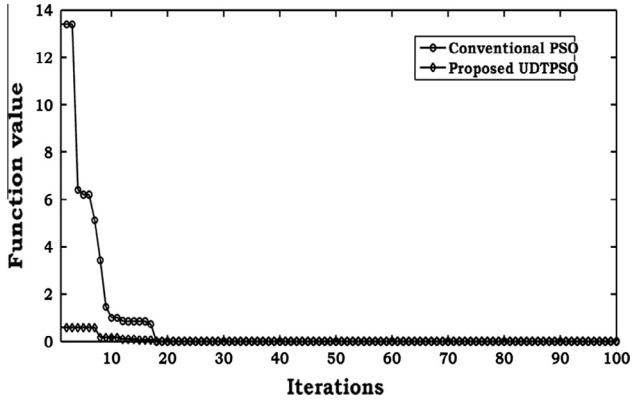


**Figure 4** Comparison of convergence characteristics of Himmelblau function.

**Table 2** Comparison of UDTPSO performance on sphere function for 100 trails.

| Function | $\sum_{i=1}^{2} X_i^2$ |
|---|---|
| Name | Sphere |
| No. of particles | 2 |
| Search space | $[-100, 100]$ |
| Worst value | 0.0035 |
| Average value | 7.4241e−004 |
| Best value | 2.0088e−006 |
| Standard deviation | 7.2195e−004 |

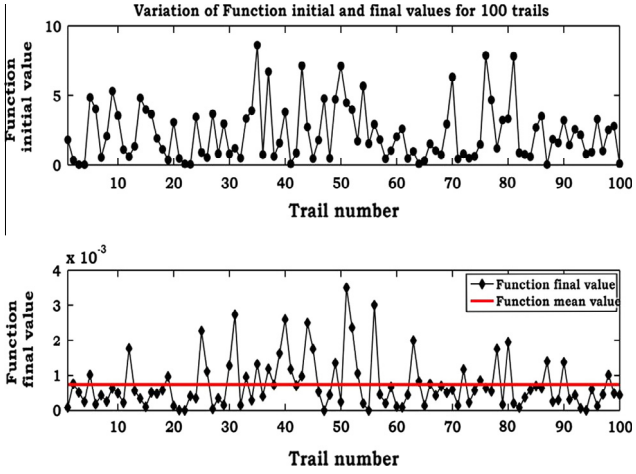


**Figure 5** Variation of sphere function initial and final values for 100 trails.

#### 6.1.1. Case-1: Generation quadratic cost function (convex cost function)

The generator cost characteristics are represented by its quadratic cost curve. This function can be expressed as:

$$FC_i = a_i P_i^2 + b_i P_i + c_i \tag{22}$$

where $a_i, b_i, c_i$ are the fuel cost-coefficients of the $i$th unit. The values of these coefficients are given in Table A1. For this system, the 2nd generator cost curve characteristics including ramp-rate and POZ effects are shown in Fig. 6.

To validate the proposed UDTPSO method, obtained generation cost is compared with the exiting PSO and TS methods and the corresponding results are tabulated in Table 3. From this table, it is observed that, with the proposed method, the cost reduction of 2.7524 \$/h and 1.6722 \$/h are obtained when compared to existing TS and PSO methods. The obtained results are validated with some of the existing literature and are tabulated in Table 4. From this table, it is observed that, the proposed method gives the best value than the existing methods. The convergence patterns for the existing PSO and proposed methods are shown in Fig. 7. From this figure, it is observed that, proposed method starts with good initial value (because of uniform distribution of control variables) and reaches best final value (because of two stage initialization process) in less number of iterations when compared to existing PSO. The uniform distribution of 2nd generator control variables for 100 iterations is shown in Fig. 8. From this figure it is observed that, the diversity of these variables is very close to each other as number of iterations is increasing. It is also observed that, in first iteration, the control variables are confined to entire solution search space, later it is confined to global best search space.

Further, the effect of considered practical constraints such as, ramp-rate and POZ limits is analyzed in four cases, and the obtained results are tabulated in Table 5.

Case-A: Without ramp-rate and without POZ.
Case-B: With ramp-rate and without POZ.
Case-C: Without ramp-rate and with POZ.
Case-D: With ramp-rate and with POZ.

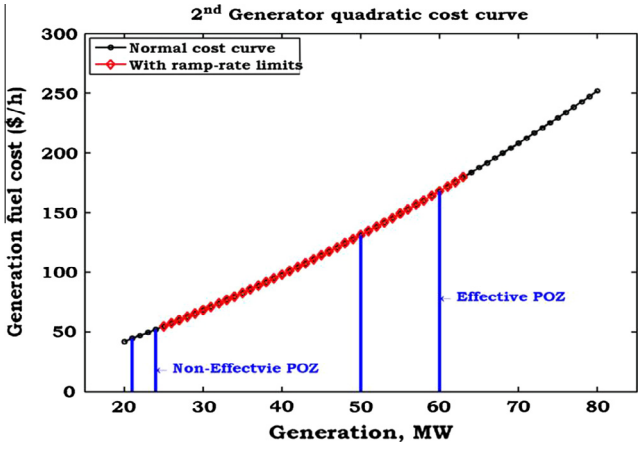


**Figure 6** Quadratic cost curve of 2nd generator in IEEE-30 bus system.

**Table 3** Comparison of OPF results for quadratic cost minimization.

| Control variable | | TS [8] | PSO | Proposed UDTPSO |
|---|---|---|---|---|
| PG1, MW | | 176.04 | 178.3828 | 177.7624 |
| PG2, MW | | 48.76 | 47.82553 | 48.9829 |
| PG5, MW | | 21.56 | 21.83552 | 21.0188 |
| PG8, MW | | 22.05 | 20.15342 | 21.02163 |
| PG11, MW | | 12.44 | 12.46363 | 11.43384 |
| PG13, MW | | 12 | 12 | 12 |
| VG1, p.u. | | 1.0500 | 1.1 | 1.1 |
| VG2, p.u. | | 1.0389 | 0.98322 | 1.087706 |
| VG5, p.u. | | 1.0110 | 1.047196 | 1.061636 |
| VG8, p.u. | | 1.0198 | 1.1 | 1.069037 |
| VG11, p.u. | | 1.0941 | 0.960144 | 1.007715 |
| VG13, p.u. | | 1.0898 | 1.027252 | 1.099918 |
| Tap 6-9, p.u. | | 1.0407 | 1.016406 | 0.97872 |
| Tap 6-10, p.u. | | 0.9218 | 1.098762 | 0.957272 |
| Tap 4-12, p.u. | | 1.0098 | 1.031778 | 0.99571 |
| Tap 28-27, p.u. | | 0.9402 | 0.994868 | 0.975997 |
| Qc 10, p.u. | | – | 27.1497 | 19.49261 |
| Qc 24, p.u. | | – | 20.98052 | 15.07354 |
| Quadratic cost ($/h) | Best | 802.29 | 801.2098 | 799.5376 |
| | Average | NA | 804.5299 | 800.141 |
| | Worst | NA | 819.5471 | 804.9866 |
| TPL, MW | | NA | 9.260945 | 8.819618 |
| Time (s) | | NA | 30.45271 | 21.66243 |

**Table 4** Summary and validation of OPF results for quadratic cost minimization.

| S. No | Method | Quadratic cost ($/h) |
|---|---|---|
| 1 | EP [52] | 803.754 |
| 4 | PSO [27] | 800.41 |
| 5 | Improved GA [4] | 800.805 |
| 6 | MDE [10] | 802.376 |
| 7 | Gradient method [53] | 804.853 |
| 8 | EADDE [54] | 800.2041 |
| 9 | EADHDE [55] | 800.1579 |
| 10 | Enhanced GA [56] | 802.06 |
| 11 | Proposed UDTPSO | 799.5376 |

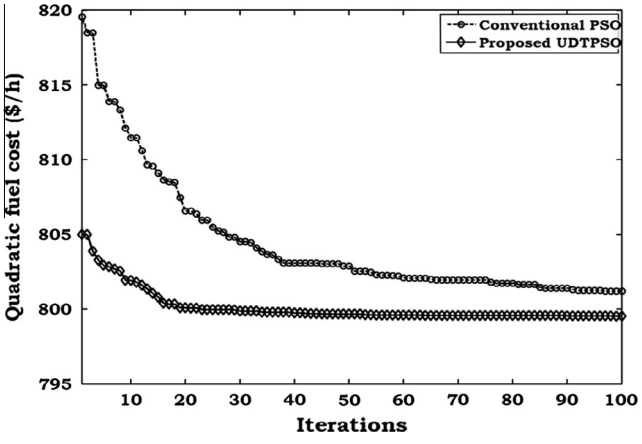


**Figure 7** Comparison of convergence characteristics of quadratic cost.

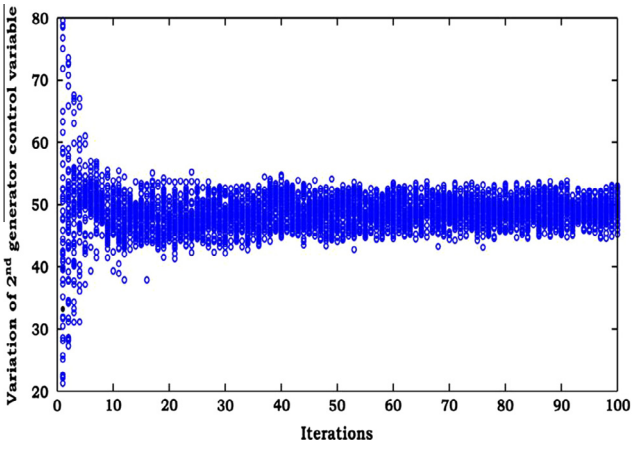


**Figure 8** Iteration-wise distribution of 2nd generator control variables.

The ramp-rate and POZ limits followed by the generators are tabulated in Table 6. From these tables, it is clearly observed that, there is an effect of practical constraints on generator characteristics. The obtained results for the fuel cost in the presence of ramp-rate and POZ limits are validated with some of the existing literature and are tabulated in Table 7. From this table, it is observed that, the proposed method gives the best value than the existing methods. The convergence characteristics for these cases are shown in Fig. 9. From this figure, it is observed that, the iterative process initial value is increasing as the number of constraints is increasing. It is also observed that, in all these cases, the iterative process reaches final best value in less than 40 iterations.

**Table 5** Comparison of OPF results for quadratic cost minimization in the presence of practical constraints for four cases.

| Control variable | Case-A | Case-B | Case-C | Case-D |
|---|---|---|---|---|
| PG1, MW | 177.7624 | 175.9465 | 176.5707 | 174.8563 |
| PG2, MW | 48.9829 | 48.04176 | 48.10696 | 48.20543 |
| PG5, MW | 21.0188 | 21.39244 | 21.69975 | 21.58456 |
| PG8, MW | 21.02163 | 19.9913 | 21.79422 | 21.13414 |
| PG11, MW | 11.43384 | 13 | 12.47445 | 13.00708 |
| PG13, MW | 12 | 14 | 12.05295 | 14 |
| VG1, p.u. | 1.1 | 1.079895 | 1.08192 | 1.069923 |
| VG2, p.u. | 1.087706 | 1.068357 | 1.02548 | 1.038589 |
| VG5, p.u. | 1.061636 | 1.039705 | 1.034214 | 1.012481 |
| VG8, p.u. | 1.069037 | 1.049274 | 1.040158 | 1.02098 |
| VG11, p.u. | 1.007715 | 1.047178 | 1.07 | 1.040455 |
| VG13, p.u. | 1.099918 | 1.079461 | 1.069098 | 1.05 |
| Tap 6-9, p.u. | 0.97872 | 1.035364 | 1.026671 | 1.017749 |
| Tap 6-10, p.u. | 0.957272 | 0.935362 | 0.975617 | 0.976178 |
| Tap 4-12, p.u. | 0.99571 | 1.025723 | 1.011592 | 0.975001 |
| Tap 28-27, p.u. | 0.975997 | 0.980173 | 0.967758 | 0.954504 |
| Qc 10, p.u. | 19.49261 | 19.47396 | 21.39108 | 27.53183 |
| Qc 24, p.u. | 15.07354 | 12.02089 | 13.56383 | 11.79691 |
| Quadratic cost ($/h) | 799.5376 | 800.8702 | 801.7697 | 802.658 |
| TPL, MW | 8.819618 | 8.972009 | 9.299054 | 9.387534 |
| Time (s) | 21.66243 | 32.12234 | 38.77821 | 45.18272 |

### *6.1.2. Case-2: Generation quadratic cost function with valve loading effects (Non-convex cost function)*

The generator fuel cost function is obtained from the data taken from the heat-run tests, and for accurate modeling valve point loading should also be included as a sinusoidal function in the cost function. The fuel input and power output, cost function of the $i$th unit with valve loadings are given as

$$FC_i = a_i P_i^2 + b_i P_i + c_i + |e_i \times \sin(f_i \times (P_i^{\min} - P_i))| \tag{23}$$

where $a_i, b_i, c_i$ are the fuel cost-coefficients of the $i$th unit and $e_i, f_i$ are the fuel cost-coefficients of the $i$th unit with valve loading effects. For this system, the 2nd generator cost curve characteristics including ramp-rate and POZ effects are shown in Fig. 10. For this system, the generators at buses 1 and 2 are considered to have the valve loading effects. The values of these coefficients for first two generators are given in Table A1, and the coefficients for the remaining generators are same as that of Case-1. Obtained results for this case are tabulated in Table 8.

**Table 6** Ramp rates and POZ limits followed by the generators for cases A, B, C and D.

| Gen. No. | Case-A | Case-B | Case-C | Case-D |
|---|---|---|---|---|
| 1 | – | Up | 2 | Up, 2 |
| 2 | – | Up | 1 | Up, 1 |
| 5 | – | Down | 1 | Down, 1 |
| 8 | – | Down | 1 | Down, 1 |
| 11 | – | Down | 1 | Down, 1 |
| 13 | $P_{G,\ min}$ | Down | 1 | Down, 1 |

1 – Below POZ lower limit, 2 – Above POZ upper limit.
UP – following up-ramp rate, Down – following down-ramp rate.

**Table 7** Summary and validation of OPF results for quadratic cost objective minimization with practical constraints.

| S.No | Method | Quadratic cost ($/h) |
|---|---|---|
| 1 | IFEP [57] | 803.86 |
| 2 | PSO [58] | 803.52 |
| 3 | HSA [59] | 802.84 |
| 4 | Proposed UDTPSO | 802.658 |

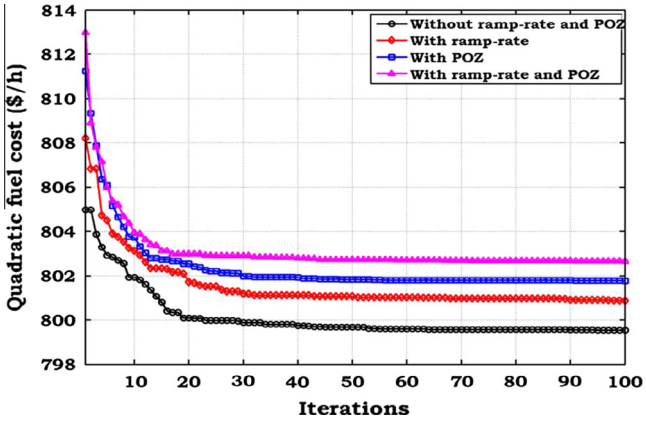


**Figure 9** Comparison of convergence characteristics of quadratic cost without and with practical constraints.

### *6.1.3. Case-3: Multi-fuel quadratic cost function*

In real time power system operation and control, many of the thermal generating stations are equipped with multiple fuel sources such as coal, natural gas, and oil. The cost curves for these generators may have the different cost coefficients. The piecewise/multi-fuel quadratic cost function can be expressed as

$$FC_i = \begin{cases} a_{i1} P_i^2 + b_{i1} P_i + c_{i1}; & P_i^{\min} \leqslant P_i \leqslant P_i^1 \\ a_{i2} P_i^2 + b_{i2} P_i + c_{i2}; & P_i^1 \leqslant P_i \leqslant P_i^2 \\ \cdots & \\ a_{ik} P_i^2 + b_{ik} P_i + c_{ik}; & P_i^{k-1} \leqslant P_i \leqslant P_i^{\max} \end{cases} \tag{24}$$

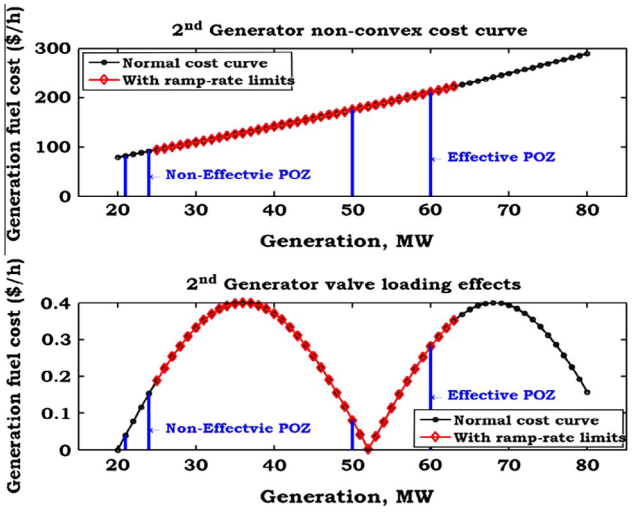


**Figure 10** Quadratic cost curve with valve loading effects of 2nd generator in IEEE-30 bus system.

where $a_{ik}, b_{ik}, c_{ik}$ are the fuel cost-coefficients of the $i$th unit for fuel type-k. The cost coefficients for the first two generators are given in Table A2. The variation of the 2nd generator multi-fuel cost curve is shown in Fig. 11. Obtained results for this case are tabulated in Table 8.

### 6.1.4. Case-4: Multi-fuel quadratic cost function with valve loading effects (Multi-fuel Non-convex cost)

In practical power system operation, thermal generating units are supplied with multiple fuels and their auxiliary equipment such as boilers is equipped with valve point effects to control power output. The more realistic cost curve including multiple fuels and its respective valve loading effects can be expressed as

$$FC_i = \begin{cases} a_{i1}P_i^2 + b_{i1}P_i + c_{i1} + |e_{i1} \times \sin(f_{i1} \times (P_i^{\min} - P_i))|; & P_i^{\min} \leqslant P_i \leqslant P_i^1 \\ a_{i2}P_i^2 + b_{i2}P_i + c_{i2} + |e_{i2} \times \sin(f_{i2} \times (P_i^{\min} - P_i))|; & P_i^1 \leqslant P_i \leqslant P_i^2 \\ \cdots \\ a_{ik}P_i^2 + b_{ik}P_i + c_{ik} + |e_{ik} \times \sin(f_{ik} \times (P_i^{\min} - P_i))|; & P_i^{k-1} \leqslant P_i \leqslant P_i^{\max} \end{cases} \tag{25}$$

where $a_{ik}, b_{ik}, c_{ik}, e_{ik}, f_{ik}$ are the fuel cost-coefficients of the $i$th unit with valve loading effects for fuel type-k. The values of these coefficients are given in Table A2. The variation of generation cost for the 2nd generator including multi-fuel and valve loading effects can be shown in Fig. 12. From this figure, it is identified that, the valve loading effects for different fuel might be different. Obtained results for this case are tabulated in Table 8.

### 6.1.5. Case-5: Total Transmission Power Loss (TPL)

In power system, the active power loss should be minimized to enhance power delivery performance and can be calculated using

$$J = TPL = \sum_{m=1}^{N_{line}} g_m \left[ V_i^2 + V_j^2 - 2V_iV_j\cos(\delta_i - \delta_j) \right] MW \tag{26}$$

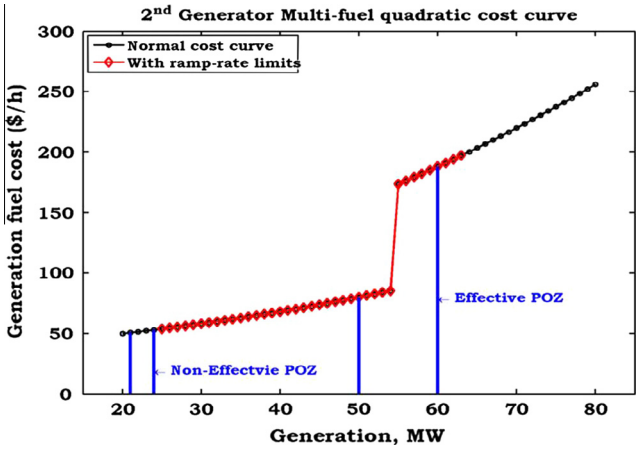


**Figure 11** Multi-fuel quadratic cost curve of 2nd generator in IEEE-30 bus system.

where '$N_{line}$' is total number of transmission lines, '$g_m$' is the conductance of $m$th line which connects buses '$i$' and '$j$'. $V_i$, $V_j$ and $\delta_i$, $\delta_j$ are voltage magnitude and angle of $i$th and $j$th buses. Obtained results for this case are tabulated in Table 8.

### 6.1.6. Case-6: Minimization of fuel cost and TPL

The aim of this type of problem is to minimize the total fuel cost and TPL simultaneously while satisfying all constraints and it is formulated as follows: [60]

$$J = \sum_{i=1}^{NG} a_iP_{G_i}^2 + b_iP_{G_i} + c_i + \left| e_i \times \sin\left( f_i \times \left( P_{G_i}^{\min} - P_{G_i} \right) \right) \right| + \frac{FC}{P_d} \times TPL \tag{27}$$

**Table 8** Comparison of OPF results for cases 2, 3, 4, 5 and 6 for without and with practical constraints for IEEE-30 bus system.

| Control variable | Case-2 | | | Case-3 | | Case-4 | | Case-5 | | Case-6 | |
|---|---|---|---|---|---|---|---|---|---|---|---|
| | TS [8] | Without | With | Without | With | Without | With | Without | With | Without | With |
| PG1, MW | 200.00 | 192.9751 | 191.9855 | 139.9813 | 139.9864 | 139.8217 | 139.9396 | 51.34983 | 82.12314 | 81.22057 | 98.49953 |
| PG2, MW | 39.65 | 42.04204 | 39.26563 | 54.93806 | 50 | 54.95776 | 50 | 80 | 63 | 54.9837 | 50 |
| PG5, MW | 20.42 | 19.96234 | 20.02186 | 23.55821 | 25.55859 | 25.71689 | 26.78133 | 49.99966 | 49 | 50 | 49 |
| PG8, MW | 12.47 | 16.83401 | 15 | 34.41323 | 30 | 25.6556 | 25 | 35 | 30 | 35 | 30 |
| PG11, MW | 10.00 | 10.01554 | 13 | 19.44754 | 21.45031 | 19.46511 | 24.47651 | 30 | 28 | 30 | 25 |
| PG13, MW | 12.00 | 12.01089 | 14 | 18.00646 | 23.61184 | 24.92612 | 24 | 40 | 35 | 35.68889 | 35 |
| VG1, p.u. | 1.05 | 1.082987 | 1.09665 | 1.093433 | 1.067075 | 1.081011 | 1.068304 | 1.1 | 1.1 | 1.099967 | 1.1 |
| VG2, p.u. | 1.0342 | 1.058762 | 1.041058 | 1.009973 | 0.983353 | 1.011849 | 1.05429 | 1.098277 | 1.026681 | 1.007843 | 1.032285 |
| VG5, p.u. | 1.0118 | 1.020481 | 1.072164 | 1.042341 | 1.014593 | 1.035938 | 1.020323 | 1.08068 | 1.077312 | 1.076726 | 1.076982 |
| VG8, p.u. | 1.0185 | 1.068426 | 1.066606 | 1.057513 | 1.040494 | 1.036927 | 1.033486 | 1.08905 | 1.072681 | 1.097245 | 1.081166 |
| VG11, p.u. | 1.0868 | 1.031774 | 1.059097 | 1.059239 | 1.005428 | 1.027438 | 1.047493 | 0.996508 | 1.038465 | 1.024713 | 1.034994 |
| VG13, p.u. | 1.0942 | 0.992062 | 1.06536 | 1.029953 | 0.991226 | 1.04537 | 1.051766 | 1.099818 | 1.1 | 1.1 | 1.1 |
| Tap 6-9, p.u. | 0.9993 | 1.091536 | 1.030682 | 1.055177 | 1.041806 | 0.961401 | 1.008546 | 1.010603 | 0.973144 | 0.987749 | 1.010529 |
| Tap 6-10, p.u. | 1.0017 | 0.992947 | 1.044612 | 0.981692 | 1.000813 | 0.961715 | 0.984092 | 0.964953 | 0.989799 | 0.983118 | 0.930768 |
| Tap 4-12, p.u. | 1.0184 | 1.000026 | 1.034351 | 1.003243 | 1.000879 | 1.00518 | 1.004904 | 0.994236 | 0.975125 | 0.973374 | 0.971699 |
| Tap 28-27, p.u. | 0.9586 | 1.022707 | 1.004656 | 0.994089 | 0.988386 | 0.974407 | 1.001898 | 0.970434 | 0.964664 | 0.965564 | 0.967176 |
| Qc 10, p.u. | – | 15.9861 | 20.02583 | 24.34213 | 17.74326 | 18.32053 | 15.22686 | 28.28745 | 24.9794 | 30 | 26.45441 |
| Qc 24, p.u. | – | 15.33373 | 12.61963 | 13.24154 | 15.47772 | 20.39457 | 13.65292 | 13.42331 | 11.96349 | 11.46897 | 12.29822 |
| Fuel cost ($/h) | 919.72 | 917.9846 | 918.2415 | 647.5118 | 662.991 | 651.8872 | 664.2395 | 963.4638 | 887.7182 | 813.3425 | 783.2371 |
| TPL | | 10.43989 | 9.873033 | 6.94476 | 7.207161 | 7.143211 | 6.797426 | 2.949494 | 3.723141 | 3.493157 | 4.098989 |
| Case-6 VALUE | – | – | – | – | – | – | – | – | – | 1815.859 | 1916.081 |

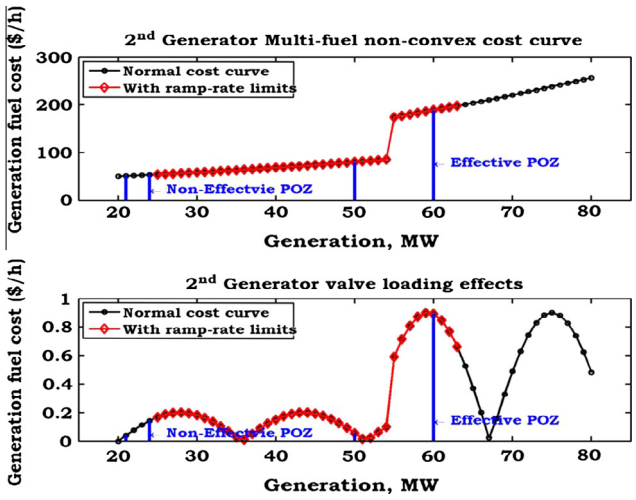


**Figure 12** Quadratic cost curve of 2nd generator in IEEE-30 bus system.

The optimized control variables and respective results for the cases 2, 3, 4, 5, and 6 are tabulated in Table 8. The effect of practical constraints on these objectives is tabulated in Table 9. From these tables, it is observed that, the objective function value is increased in the presence of practical constraints. The multi-fuel generation cost is increased from 649.6987 $/h in case-3 to 651.8872 $/h in case-4, because of valve loading effects for without practical constraints and this value is increased from 662.991 $/h in case-3 to 664.2395 $/h in case-4 in the presence of practical constrains. In case-4, the transmission power losses are reduced by 0.40974 MW when compared to without and with practical constraints. In case-5, the losses are increased from 2.9494 MW to 3.7231 MW in the presence of practical constrains, conversely the generation cost is decreased by 75.7456 $/h.

In case-6, multi-objective optimization problem by combining multi-fuel non-convex cost (MFNCC) and transmission power loss (TPL) objectives are optimized using Eq. (12). From this table, it is observed that, based on the system loading conditions, generation cost and TPL values are optimized and obtained within its individual minimization limits. From this analysis it is summarized that, there is an effect of valve loadings and practical constraints on multi-fuel generation cost and transmission losses.

The obtained results for the Non-convex fuel and multi-fuel quadratic costs without ramp-rate and POZ limits are validated with some of the existing literature and are tabulated in Tables 10 and 11. From these tables, it is observed that, the proposed method gives the best value than the existing methods.

To show the effect of practical constraints clearly, the variation of active power generation control variables for case-4 is shown in Fig. 13. From this figure it is observed that, the control variables (Pg1–Pg6) are characterized by their practical constraints. In Fig. 13(a) it is in continuously distorting manner while in Fig. 13(b), it is in smooth manner.

Here to show the effect of UPFC, initially the formulated severity function given in Eq. (17) is optimized. The optimal location to install UPFC is identified by performing the procedure described in Section 3.1. The result of contingency analysis for this system is given in Table 12. To maintain the continuity in supplying/receiving the power, the contingency analysis is not performed for lines between buses 9–11, 12–13, and 25–26. Hence, for this system only 38 transmission line

**Table 9** Ramp rates and POZ limits followed by the generators for cases 2, 3, 4, 5 and 6.

| Gen. No. | Case-2 | Case-3 | Case-4 | Case-5 | Case-6 |
|---|---|---|---|---|---|
| 1 | Up, 2 | Down, 2 | Down, 2 | Down, 1 | Down, 1 |
| 2 | Up, 1 | Up, 3 | Up, 3 | Up, 2 | Up, 3 |
| 5 | Down, 1 | Down, 1 | Down, 1 | Up, 2 | Up, 2 |
| 8 | Down, 1 | Up, 4 | Up, 3 | Up, 4 | Up, 4 |
| 11 | Down, 1 | Up, 1 | Up, 1 | Up, 4 | Up, 3 |
| 13 | Down, 1 | Up, 1 | Up, 3 | Up, 2 | Up, 2 |

1 – Below POZ lower limit, 2 – Above POZ upper limit.
3 – Equal to POZ lower limit, 4 – Equal to POZ upper limit.
UP – following up-ramp rate, Down – following down-ramp rate.

**Table 10** Summary and validation of OPF results for quadratic cost with valve loading effects objective minimization.

| S.No | Method | Non-convex cost |
|---|---|---|
| 1 | BBO [61] | 919.7647 |
| 2 | GSA [62] | 929.72404 |
| 3 | MDE [10] | 930.793 |
| 4 | Proposed UDTPSO | 917.9846 |

**Table 11** Summary and validation of OPF results for multi-fuel quadratic cost objective minimization.

| S.No | Method | Multi-fuel quadratic cost |
|---|---|---|
| 1 | BBO [61] | 647.7437 |
| 2 | DE [9] | 650.8224 |
| 3 | PSO [27] | 647.69 |
| 4 | MDE [10] | 647.846 |
| 5 | Proposed UDTPSO | 647.5118 |

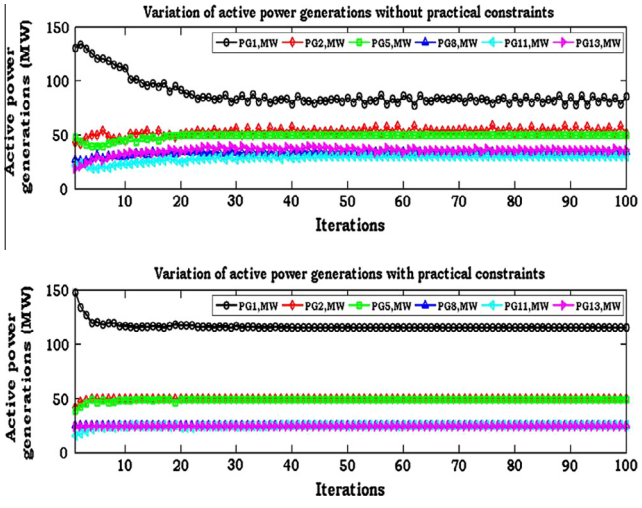


**Figure 13** Variation of active power generation control variables in case-4 for without and with practical constraints.

**Table 12** Results of contingency ranking.

| S. No. | Line No | Outage Line | Overloaded lines (Line flow/MVA limit) | Noll | Voltage violated buses | NVVB | PI | Rank |
|---|---|---|---|---|---|---|---|---|
| 1 | 5 | 2–5 | (1–2) (171.399/130)<br>(2–4) (77.671/65)<br>(2–6) (105.434/65)<br>(4–6) (121.418/90)<br>(5–7) (110.190/70)<br>(6–8) (35.828/32) | 6 | – | 0 | 6 | 1 |
| 2 | 36 | 28–27 | (1–2) (180.949/130)<br>(22–24) (20.246/16)<br>24–25) (19.501/16) | 3 | 27 (0.8989)<br>29 (0.8760)<br>30 (0.8627) | 3 | 6 | 2 |

**Table 13** Severity function values under rank-1 contingency with UPFC.

| S. No. | UPFC location | | Severity function value |
|---|---|---|---|
| | Sending end bus | Receiving end bus | |
| 1 | 12 | 14 | 1.608 |
| 2 | 30 | 27 | 1.6479 |
| 3 | 15 | 14 | 1.6484 |
| 4 | 27 | 25 | 1.6503 |
| 5 | 6 | 4 | 1.6573 |

contingencies out of 41 are considered. The result of only top 2 contingencies is tabulated.

From Table 12, it is very clear that, the line connected between buses 2 and 5 is the most critical one. By following above rules given in Section-3, the possible UPFC installation locations are 38. Severity function is evaluated in all locations with UPFC and the top 5 least severe function valued locations are tabulated in Table 13 under rank-1 contingency.

From Table 13, it is observed that, first location is the best location for placing the UPFC, because it has least severity function value. The further analysis is performed by placing device in this location.

The analysis is performed to identify the effect of UPFC on the considered objectives. The OPF results for cases 4, 5, and 6

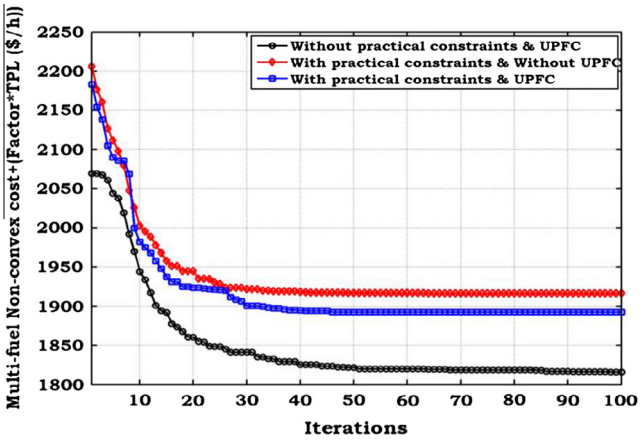


**Figure 14** Comparison of convergence characteristics in the presence of UPFC under normal condition in case-6 for without and with practical constraints.

under normal, single line (2–5) and double line (2–5, 28–27) contingency cases are tabulated in Table 14. From this table, it is observed that, minimizing one of the objectives sacrifices the other objectives. It is observed that, in the presence of practical constraints and in contingency conditions, the objective function values are increased. Finally, with UPFC, the single

**Table 14** Comparison of OPF results for normal, single line and double line contingency conditions for without and with practical constraints.

| Case | | Objectives | Normal | | Single line contingency | | Double line contingency | |
|---|---|---|---|---|---|---|---|---|
| | | | Without | With | Without | With | Without | With |
| Without | Case-4 | MFNCC | 651.8872 | 664.2395 | 669.9045 | 686.3319 | 680.3726 | 700.0991 |
| | | TPL | 7.143211 | 6.797426 | 11.89348 | 11.66354 | 13.04804 | 12.62619 |
| | Case-5 | MFNCC | 963.4638 | 887.7182 | 966.6805 | 892.1422 | 903.9518 | 839.5114 |
| | | TPL | 2.949494 | 3.723141 | 5.437907 | 6.517208 | 9.132667 | 10.64863 |
| | Case-6 | Function value | 1815.859 | 1916.081 | 2557.224 | 2742.985 | 3024.328 | 3120.327 |
| | | MFNCC | 813.3425 | 783.2371 | 827.6603 | 786.0787 | 833.5588 | 790.3732 |
| | | TPL | 3.493157 | 4.098989 | 5.922217 | 7.05511 | 7.448351 | 8.354394 |
| UPFC | Case-4 | MFNCC | 649.6137 | 663.6464 | 666.097 | 685.9325 | 678.2233 | 699.0834 |
| | | TPL | 7.263833 | 6.897366 | 13.06038 | 11.78724 | 13.51211 | 12.72169 |
| | Case-5 | MFNCC | 963.4891 | 887.4848 | 968.8229 | 899.2809 | 882.9286 | 858.5399 |
| | | TPL | 2.891629 | 3.700542 | 5.374356 | 6.353759 | 9.116038 | 10.52589 |
| | Case-6 | Function value | 1790.798 | 1892.254 | 2531.34 | 2683.386 | 2974.724 | 3103.935 |
| | | MFNCC | 814.2064 | 780.4159 | 831.2264 | 785.6935 | 833.4822 | 781.7124 |
| | | TPL | 3.399213 | 4.037525 | 5.796402 | 6.844987 | 7.280635 | 8.890224 |

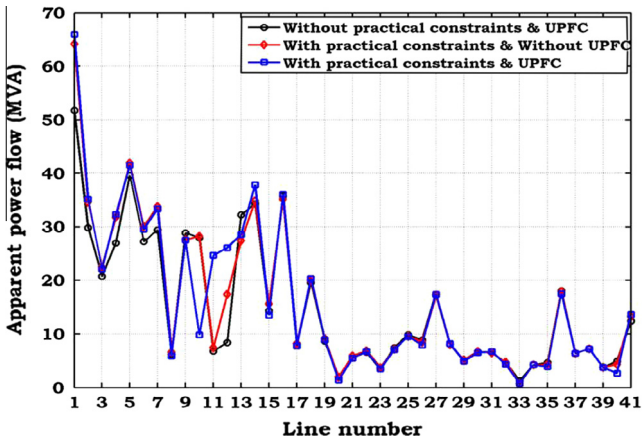


**Figure 15** Variation of active power flow in lines in the presence of UPFC under normal condition in case-6 for without and with practical constraints.

and multi-objective optimization problems are optimized and are enhanced under normal and contingency conditions when compared to without device. The convergence characteristics for case-6 are shown in Fig. 14. From this figure, it is observed that, with UPFC and in the presence of practical constraints, the iterative process starts with good initial value and obtained better convergence characteristics when compared to without device. The variation of the apparent power flows in the presence of UPFC is shown in Fig. 15. From this figure, it is noticed that, the power flow is diverted through lines 11 (6–9) and 12 (6–10) because of the presence of tap setting transformers instead of 8 (5–7). It is also observed that, power flow variations are obtained in the lines nearer to the device connected location.

### *6.2. Example-2*

To extend the effectiveness of the proposed methodology, tamilnadu-62 bus system with 89 lines is considered [63]. The total control variables in this system are 49. The cost coefficients for quadratic, non-convex and multi-fuel costs are given in Tables A3 and A4. Due to space restrictions, the OPF results without UPFC with active power generation control variables are tabulated in Table 15. From this table, the similar observations can be interpreted as in example-1.

## 7. Conclusion

In this paper, a novel optimization algorithm based on uniform distribution of control variables and two-stage initialization processes in conventional PSO has been proposed to solve OPF problem. The objectives such as conventional quadratic, non-convex costs and multi-fuel quadratic, non-convex costs are optimized while satisfying equality, inequality and practical constraints. The effect of multi-fuel on economic load dispatch has been presented with respective validations. The effect of practical constraints such as ramp-rate and POZ limits has been analyzed on the defined objectives. It is concluded that, using the proposed UDTPSO, best objective

**Table 15** Comparison of OPF results for all cases for without and with practical constraints for Indian-62 bus system.

| Control variable | Case-1 | | Case-2 | | Case-3 | | Case-4 | | Case-5 | | Case-6 | |
|---|---|---|---|---|---|---|---|---|---|---|---|---|
| | Without | With | Without | With | Without | With | Without | With | Without | With | Without | With |
| PG1 | 62.84395 | 178.1201 | 256.7089 | 269.3694 | 157.4156 | 144.9591 | 238.4362 | 226.0235 | 281.9596 | 147.9991 | 251.7562 | 287.7347 |
| PG2 | 226.3074 | 204.8721 | 245.2081 | 253.2243 | 242.543 | 241.7627 | 239.5133 | 244.9003 | 192.6162 | 312.3889 | 241.9397 | 229.1803 |
| PG5 | 269.291 | 290 | 246.7826 | 250 | 248.0004 | 250.2374 | 250 | 250 | 233.769 | 250 | 218.38 | 200 |
| PG9 | 100 | 46.49528 | 17.04873 | 14.16873 | 38.53341 | 76.73015 | 20.97844 | 17.53986 | 20.73626 | 12.53121 | 19.87155 | 18.00571 |
| PG14 | 200.2826 | 194.9787 | 55.79072 | 58.66968 | 198.3589 | 136.4353 | 53.00234 | 56.92066 | 58.99504 | 56.71781 | 55.89784 | 56.85449 |
| PG17 | 267.3617 | 139.0095 | 258.5341 | 197.2661 | 248.3751 | 252.0527 | 226.2347 | 199.8762 | 188.3961 | 200 | 201.7091 | 250.1909 |
| PG23 | 152.5738 | 100 | 53.53095 | 54.85379 | 136.5025 | 88.72254 | 56.70202 | 56.11039 | 53.35763 | 55.26965 | 60.77544 | 61.62265 |
| PG25 | 183.9104 | 318.3758 | 353.9653 | 376.244 | 273.043 | 281.2814 | 352.4963 | 406.3642 | 478.4623 | 387.8164 | 450.16 | 364.6005 |
| PG32 | 129.2219 | 267.6361 | 279.8838 | 349.5012 | 123.7085 | 200 | 276.188 | 358.2202 | 409.5176 | 407.3194 | 409.747 | 375.1018 |
| PG33 | 83.61177 | 30 | 32.98271 | 25.69971 | 97.83594 | 30 | 26.09565 | 30 | 20.74734 | 25.04595 | 23.55847 | 27.50485 |
| PG34 | 119.9931 | 150 | 136.9573 | 100 | 122.1537 | 150 | 149.4415 | 99.76187 | 85.07666 | 97.21979 | 96.18686 | 150 |
| PG37 | 50 | 19.02751 | 69.15782 | 57.24218 | 24.24226 | 25.61469 | 46.61751 | 55.06063 | 52.00272 | 47.31379 | 43.13058 | 30 |
| PG49 | 248.9817 | 137.2589 | 53.9571 | 59.62966 | 181.3891 | 200 | 62.40242 | 56.93291 | 58.84986 | 53.28536 | 58.22001 | 56.30938 |
| PG50 | 146.0361 | 85.92167 | 77.83726 | 64.83452 | 128.7132 | 99.1514 | 89.75654 | 26.49188 | 73.97933 | 73.06235 | 42.06086 | 58.84013 |
| PG51 | 126.9405 | 212.7356 | 199.7142 | 220 | 160.9392 | 154.3828 | 220 | 193.7099 | 154.7769 | 150 | 185.8271 | 151.8179 |
| PG52 | 138.2644 | 96.38393 | 71.51308 | 57.11659 | 117.1491 | 97.07804 | 78.69458 | 69.80723 | 44.98833 | 56.00961 | 34.45864 | 44.80536 |
| PG54 | 74.1645 | 50.07593 | 60.77472 | 55.06572 | 84.36429 | 69.79082 | 69.11714 | 65.78293 | 65.12345 | 71.00474 | 48.01833 | 62.2626 |
| PG57 | 283.6437 | 197.152 | 75.78781 | 68.75055 | 286.6001 | 72.44151 | 108.1123 | 102.1119 | 51.66241 | 113.2402 | 69.83553 | 100.4075 |
| PG58 | 116.4547 | 250 | 415.5484 | 429.6062 | 111.5435 | 400 | 400 | 440.987 | 428.2606 | 443.2921 | 437.9604 | 431.5099 |
| Fuel cost ($/h) | 13972.07 | 16901.25 | 19803.04 | 20873.9 | 13051.56 | 15084.01 | 17881.58 | 19197.24 | 19917.85 | 18947.44 | 19655.52 | 18804.4 |
| TPL, MW | 71.88322 | 60.04317 | 53.68363 | 53.24229 | 73.41094 | 62.64062 | 55.78892 | 48.6015 | 45.27738 | 51.51621 | 41.49373 | 48.7485 |
| Case-6 VALUE | – | – | – | – | – | – | – | – | – | – | 48409.06 | 50964.99 |

values are obtained when compared to existing methods discussed in the literature. The proposed approach has been successfully and influentially tested on standard test functions and electrical systems. The objective values in electrical systems are further enhanced in the presence of UPFC with appropriate optimal settings. Finally, this paper presents a solution methodology to optimize more realistic problem by considering multi-fuel and practical constraints on economic load dispatch. The proposed method has proved its effectiveness in terms of speed of convergence, consistency, and robustness. From this, it is very clear that, the proposed approach can be a promising approach for real-time and real-size applications.

## Appendix A

The OPF data related to the considered test systems is given in Tables A1–A4.

**Table A1** Quadratic and Non-convex cost coefficients data for IEEE-30 bus system.

| S. No | Gen No | Convex cost | | | $P^{min}$ | $P^{max}$ | Non-convex cost | | | | | Ramp-rate limits | | | POZ |
|---|---|---|---|---|---|---|---|---|---|---|---|---|---|---|---|
| | | *a* | *b* | *c* | | | *a* | *b* | *c* | *d* | *e* | UR | DR | Pi0 | |
| 1 | 1 | 0.00375 | 2 | 0 | 50 | 200 | 0.0016 | 2 | 150 | 0.5 | 0.063 | 60 | 80 | 150 | 100–120 |
| 2 | 2 | 0.0175 | 1.75 | 0 | 20 | 80 | 0.01 | 2.5 | 25 | 0.4 | 0.098 | 28 | 10 | 35 | 50–60 |
| 3 | 5 | 0.0625 | 1 | 0 | 15 | 50 | 0.0625 | 1 | 0 | 0 | 0 | 10 | 20 | 39 | 30–36 |
| 4 | 8 | 0.00834 | 3.25 | 0 | 10 | 35 | 0.00834 | 3.25 | 0 | 0 | 0 | 10 | 5 | 20 | 25–30 |
| 5 | 11 | 0.025 | 3 | 0 | 10 | 30 | 0.025 | 3 | 0 | 0 | 0 | 10 | 5 | 18 | 25–28 |
| 6 | 13 | 0.025 | 3 | 0 | 12 | 40 | 0.025 | 3 | 0 | 0 | 0 | 15 | 6 | 20 | 24–30 |

**Table A2** Multi-fuel quadratic and Multi-fuel non-convex cost coefficients data for IEEE-30 bus system.

| S. No | Gen. No. | Convex cost | | | $P^{min}$ | $P^{max}$ | Non-convex cost | | | | |
|---|---|---|---|---|---|---|---|---|---|---|---|
| | | *a* | *b* | *c* | | | *a* | *b* | *c* | *d* | *e* |
| 1 | 1 | 0.005 | 0.7 | 55 | 50 | 140 | 0.005 | 0.7 | 55 | 0.35 | 0.3 |
| | | 0.0075 | 1.05 | 82.5 | 140 | 200 | 0.0075 | 1.05 | 82.5 | 0.25 | 0.2 |
| 2 | 2 | 0.01 | 0.3 | 40 | 20 | 55 | 0.01 | 0.3 | 40 | 0.2 | 0.2 |
| | | 0.02 | 0.6 | 80 | 55 | 80 | 0.02 | 0.6 | 80 | 0.9 | 0.2 |

**Table A3** Quadratic and Non-convex cost coefficients data for Indian-62 bus system.

| S. No | Gen. No. | Convex cost | | | $pg^{min}$ | $pg^{max}$ | Non-convex cost | | | | | Ramp-rate limits | | | POZ |
|---|---|---|---|---|---|---|---|---|---|---|---|---|---|---|---|
| | | *a* | *b* | *c* | | | *a* | *b* | *c* | *d* | *e* | UR | DR | Pi0 | |
| 1 | 1 | 0.007 | 6.8 | 95 | 50 | 300 | 0.0097 | 6.8 | 119 | 90 | 0.72 | 95 | 150 | 250 | 150–200 |
| 2 | 2 | 0.0055 | 4 | 30 | 50 | 450 | 0.0055 | 4 | 90 | 79 | 0.05 | 138 | 180 | 300 | 150–200 |
| 3 | 5 | 0.0055 | 4 | 45 | 50 | 450 | 0.0055 | 4 | 45 | 0 | 0 | 100 | 200 | 300 | 200–250 |
| 4 | 9 | 0.0025 | 0.85 | 10 | 0 | 100 | 0.0025 | 0.85 | 0 | 0 | 0 | 5 | 12 | 20 | 80–85 |
| 5 | 14 | 0.006 | 4.6 | 20 | 50 | 300 | 0 | 5.28 | 0.891 | 0 | 0 | 80 | 90 | 120 | 200–250 |
| 6 | 17 | 0.0055 | 4 | 90 | 50 | 450 | 0.008 | 3.5 | 110 | 0 | 0 | 100 | 150 | 300 | 200–250 |
| 7 | 23 | 0.0065 | 4.7 | 42 | 50 | 200 | 0 | 5.439 | 21 | 0 | 0 | 70 | 100 | 130 | 100–130 |
| 8 | 25 | 0.0075 | 5 | 46 | 50 | 500 | 0.0075 | 6 | 88 | 50 | 0.52 | 400 | 500 | 600 | 200–250 |
| 9 | 32 | 0.0085 | 6 | 55 | 0 | 600 | 0.0085 | 6 | 55 | 0 | 0 | 200 | 300 | 500 | 200–250 |
| 10 | 33 | 0.002 | 0.5 | 58 | 0 | 100 | 0.009 | 5.2 | 90 | 0 | 0 | 10 | 15 | 30 | 30–40 |
| 11 | 34 | 0.0045 | 1.6 | 65 | 50 | 150 | 0.0045 | 1.6 | 65 | 0 | 0 | 55 | 85 | 100 | 100–150 |
| 12 | 37 | 0.0025 | 0.85 | 78 | 0 | 50 | 0.0025 | 0.85 | 78 | 58 | 0.02 | 25 | 25 | 50 | 30–40 |
| 13 | 49 | 0.005 | 1.8 | 75 | 50 | 300 | 0 | 2.55 | 49 | 0 | 0 | 80 | 90 | 120 | 200–250 |
| 14 | 50 | 0.0045 | 1.6 | 85 | 0 | 150 | 0.0045 | 1.6 | 85 | 0 | 0 | 40 | 45 | 50 | 100–120 |
| 15 | 51 | 0.0065 | 4.7 | 80 | 0 | 500 | 0.0065 | 4.7 | 80 | 92 | 0.75 | 95 | 105 | 125 | 100–150 |
| 16 | 52 | 0.0045 | 1.4 | 90 | 50 | 150 | 0.0045 | 1.4 | 90 | 0 | 0 | 25 | 40 | 55 | 100–120 |
| 17 | 54 | 0.0025 | 0.85 | 10 | 0 | 100 | 0.0025 | 0.85 | 10 | 0 | 0 | 25 | 40 | 55 | 30–40 |
| 18 | 57 | 0.0045 | 1.6 | 25 | 50 | 300 | 0.0045 | 1.6 | 25 | 0 | 0 | 80 | 100 | 150 | 80–100 |
| 19 | 58 | 0.008 | 5.5 | 90 | 100 | 600 | 0.008 | 5.5 | 90 | 0 | 0 | 100 | 150 | 550 | 250–300 |

**Table A4** Multi-fuel quadratic and Multi-fuel non-convex cost coefficients data for Indian-62 bus system.

| S. No | Gen. No. | Convex cost | | | $pg^{min}$ | $pg^{max}$ | Non-convex cost | | | | |
|---|---|---|---|---|---|---|---|---|---|---|---|
| | | *a* | *b* | *c* | | | *a* | *b* | *c* | *d* | *e* |
| 1 | 1 | 0.005 | 3.2 | 45 | 100 | 180 | 0.005 | 3.2 | 45 | 0.25 | 0.25 |
| | | 0.0045 | 6.1 | 60.5 | 180 | 300 | 0.0045 | 6.1 | 60.5 | 0.9 | 0.15 |
| 2 | 2 | 0.0045 | 2.15 | 35.5 | 120 | 250 | 0.0045 | 2.15 | 35.5 | 0.31 | 0.0454 |
| | | 0.00255 | 4.48 | 54.5 | 250 | 438 | 0.00255 | 4.48 | 54.5 | 0.562 | 0.0542 |
| 3 | 8 | 0.0035 | 3.55 | 50.5 | 100 | 300 | 0.0035 | 3.55 | 50.5 | 0.65 | 0.1002 |
| | | 0.0055 | 5.51 | 30.5 | 300 | 500 | 0.0055 | 5.51 | 30.5 | 0.26162 | 0.0542 |
| 4 | 12 | 0.035 | 5.25 | 40.5 | 25 | 50 | 0.035 | 5.25 | 40.5 | 0.543 | 0.1421 |
| | | 0.0055 | 8.41 | 50.5 | 50 | 75 | 0.0055 | 8.41 | 50.5 | 0.5543 | 0.1234 |
| 5 | 15 | 0.0055 | 4.25 | 60 | 20 | 120 | 0.0055 | 4.25 | 60 | 0.453 | 0.0843 |
| | | 0.0045 | 3.41 | 50.5 | 120 | 220 | 0.0045 | 3.41 | 50.5 | 0.645 | 0.0652 |

## References


[1] Momoh JA, El-Hawary ME, Adapa R. A review of selected optimal power flow literature to, Part-I: Nonlinear and quadratic programming approaches. IEEE Trans Power Syst 1993;14(1999):96–104.

[2] Momoh JA, El-Hawary ME, Adapa R. A review of selected optimal power flow literature to, Part-II: Newton, linear programming and interior point methods. IEEE Trans Power Syst 1993;14(1999):105–11.

[3] Khorsandi A, Alimardani A, Vahidi B, Hosseinian SH. Hybrid shuffled frog leaping algorithm and Nelder-Mead simplex search for optimal reactive power dispatch. IEE Proc Gener Trans Distrib 2011;5:249–56.

[4] Lai LL, Ma JT, Yokoyama R, Zhao M. Improved genetic algorithm for optimal power flow under both normal and contingent operation states. Electric Power Energy Syst 1997;19:287–92.

[5] Bakirtzis AG, Biskas PN, Zoumas CE, Petridis V. Optimal power flow by enhanced genetic algorithm. IEEE Trans Power Syst 2002;17:229–36.

[6] Roa-Sepulveda CA, Pavez-Lazo BJ. A solution to the optimal power flow using simulated annealing. Electric Power Energy Syst 2003;25:47–57.

[7] Sousa T, Soares J, Vale ZA, Morais H, Faria P. Simulated annealing metaheuristic to solve the optimal power flow. IEEE Power Energy Soc General Meet 2011:1–8.

[8] Abido MA. Optimal power flow using tabu search algorithm. Electric Power Component Syst 2002;30:469–83.

[9] Abou El-Ela AA, Abido MA, Spea SR. Optimal power flow using differential evolution algorithm. Electric Power Syst Res 2010;80:878–85.

[10] Sayah S, Sehar K. Modified differential evolution algorithm for optimal power flow with non-smooth cost functions. Energy Convers Manage 2008;49:3036–42.

[11] Nayak MR, Krishnanand KR, Rout PK. Modified differential evolution optimization algorithm for multi-constraint optimal power flow. Int Conf Energy Autom Signal 2011:1–7.

[12] Sivasubramani S, Swarup KS. Multi-objective harmony search algorithm for optimal power flow problem. Electrical Power Energy Syst 2011;33:745–52.

[13] Roy PK, Ghoshal SP, Thakur SS. Biogeography based optimization for multi constrain optimal power flow with emission and non-smooth cost function. Expert Syst Appl 2010;37:8221–8.

[14] Rarick R, Simon D, Villaseca FE, Vyakaranam B. Biogeographic based optimization and the solution of the power flow problem. IEEE Int Conf Syst Man Cyber 2009:1003–8.

[15] Yang HT, Yang PC, Huang CL. Evolutionary programming based economic dispatch for units with non-smooth incremental fuel cost function. IEEE Trans Power Syst 1996;11(1):112–8.

[16] Sinha N, Chakrabarti R, Chattopadhyay PK. Evolutionary programming techniques for economic load dispatch. IEEE Trans Evol Comput 2003;7(1):83–94.

[17] Basu M. Artificial immune system for dynamic economic dispatch. Electrical Power Energy Syst 2011;33(1):131–6.

[18] Leea Jia-Chu, Lina Whei-Min, Liaob Gwo-Ching. Quantum genetic algorithm for dynamic economic dispatch with valve-point effects and including wind power system. Electrical Power Energy Syst 2011;33(2):189–97.

[19] Immanuel Selvakumar A. Enhanced cross-entropy method for dynamic economic dispatch with valve-point effects. Electrical Power Energy Syst 2011;33(3):783–90.

[20] Giang ZL. Particle swarm optimization to solving the economic dispatch considering generator constraints. IEEE Trans Power Syst 2003;18(3):1718–27.

[21] Park JB, Lee KS, Shin JR, Lee KY. A particle swarm optimization for economic dispatch with non smooth cost functions. IEEE Trans Power Syst 2005;20(1):34–42.

[22] Jeyakumar DN, Jayabarathi T, Raghunathan T. Particle swarm optimization for various types of economic dispatch problems. Electrical Power Energy Syst 2005;28(1):36–42.

[23] Selvakumar AI, Thanushkodi K. A new particle swarm optimization solution to Nonconvex economic dispatch problems. IEEE Trans Power Syst 2007;22(1):42–51.

[24] Ratnaweera A, Halgamuge SK, Watson HC. Self-organizing hierarchical particle swarm optimizer with time varying acceleration coefficients. IEEE Trans Evol Comput 2004;8:240–55.

[25] Niknam T, DoagouMojarrad H, ZeinoddiniMeymand H. A novel hybrid particle swarm optimization for economic dispatch with valve point loading effects. Energy Convers Manage 2011;52(4):1800–9.

[26] Kennedy J, Eberhart R. Particle swarm optimization. IEEE Int Conf Neural Network 1995;4:1942–8.

[27] Abido MA. Optimal power flow using particle swarm optimization. Electrical Power Energy System 2002;24:563–71.

[28] Park JB, Jeong YW, Kim HH, Shin JR. An improved particle swarm optimization for economic dispatch with valve-point effect. Int J Innov Energy Syst Power 2006;1(1):1–7.

[29] Caponetto R, Fortuna L, Fazzino S, Xibilia MG. Chaotic sequences to improve the performance of evolutionary algorithms. IEEE Trans Evol Comput 2003;7(3):289–304.

[30] Naresh Babu AV, Ramana T, Sivanagaraju S. Analysis of optimal power flow problem based on two stage initialization algorithm. Int J Electr Power Energy Syst 2014;55:91–9.

[31] Douglas JG, Heydt GT. Power flow control and power flow studies for systems with FACTS devices. IEEE Trans Power Syst 1998;13(1):60–5.

[32] Povh D. Modeling of FACTS in power system studies. IEEE Power Eng Soc Winter Meet 2000;2:1435–9.

[33] Fuerte-Esquivel CR, Acha E. Unified power flow controller: a critical comparison of Newton-Raphson UPFC algorithms in power flow studies. IEE Proc Gen Trans Distr 1997;144(5):437–44.
[34] Singh SN, Erlich I. Locating unified power flow controller for enhancing power system loadability. Int Conf Future Power Syst 2005:1–5.
[35] Wang KP, Yurevich J, Li A. Evolutionary programming based load flow algorithm for systems containing unified power flow controller. IEE Proc Gen Trans Distrib 2003;150:441–6.
[36] Arabkhaburi D, Kazemi A, Yari M, Aghaei J. Optimal placement of UPFC in power systems using genetic algorithm. IEEE Int Conf Ind Technol 2006:1694–9.
[37] Saravanan M, Mary Raja Slochanal S, Venkatesh P, Prince Stephen Abraham J. Application of PSO technique for optimal location of FACTS devices considering system loadability and cost of installation. Electrical Power Syst Res 2007;77:276–83.
[38] Sobajic D, Pao Y. An artificial intelligence system for power system contingency screening. IEEE Trans Power Syst 1988;3:647–53.
[39] Ejebe C et al. Fast contingency screening and evaluation for voltage stability analysis. IEEE Trans Power Syst 1988;3:1582–8.
[40] Chen R et al. Multi-contingency preprocessing for security analysis using physical concepts and CQR with classifications. IEEE Trans Power Syst 1993;8:840–6.
[41] Song SH, Lim JU, Jung SW, Moon SI. Preventive and corrective operation of FACTS devices to cope with a single line-faulted contingency. IEEE PES Gen Meet 2004:837–42.
[42] Sudersan A. Abdelrahman M, Radman G. Contingency selection and static security enhancement in power systems using Heuristics based genetic algorithms. In: IEEE Proc. thirty sixth southeastern symposium; 2004. p. 556–60.
[43] Basu M. Optimal power flow with FACTS devices using differential evolution. Electrical Power Energy Syst 2008;30:150–6.
[44] Tumay M, Vuram AM, Lo KL. The effect of unified power flow controller in power systems. Electrical Power Energy Syst 2004;26:561–9.
[45] Vural AM, Tumay M. Mathematical modeling and analysis of a unified power flow controller: a comparison of two approaches in power flow studies and effects of UPFC location. Electrical Power Energy Syst 2007;29:617–29.
[46] Shaheen Husam I, Rahed Ghamgeen I, Cheng SJ. Optimal location and parameter setting of UPFC for enhancing power system security based on Differential Evolution algorithm. Electrical Power Energy Syst 2011;33:94–105.
[47] Univariate Distribution Relationships., <http://www.math.wm.edu/~leemis/chart/UDR/UDR.html>.
[48] Uniform distribution, <http://mathworld.wolfram.com/UniformDistribution.html>.
[49] Deb K. Optimization for engineering design: algorithms and examples. PHI; May 2009. p. 303–16.
[50] Alsac O, Stott B. Optimal load flow with steady state security. IEEE PES summer meeting & EHV/UHV conference; 1973. p. 745–51.
[51] Arul R, Ravi G, Velsami S. Non-convex economic dispatch with heuristic load patterns, valve point loading effect, prohibited operating zones, ramp-rate limits, and spinning reserve constraints using harmony search algorithm. Electr. Eng. 2013;95:53–61.
[52] Gnanadass R, Padhy Narayana Prasad, Manivannan K. Assessment of available transfer capability for practical power system with combined economic emission dispatch. Electric Power Syst Res 2004;69:267–76.
[53] Lee KY, Park YM, Ortiz JL. A united approach to optimal real and reactive power dispatch. IEEE Trans Power Appar Syst 1985;104(5):1147–53.
[54] Vaisakh K, Srinivas LR. Evolving ant direction differential evolution for OPF with non-smooth cost functions. Eng Appl Artif Intell 2011;24:426–36.
[55] Vaisakh K, Srinivas LR. Genetic evolving ant direction HDE for OPF with non-smooth cost functions and statistical analysis. Expert Syst Appl 2011;38:2046–62.
[56] Bakirtzis AG, Biskas PN, Zournas CE, Petridis V. "Optimal power flow by enhanced genetic algorithm". IEEE Trans Power Syst 2002;17(2):229–36.
[57] Sinha N, Chakrabarti R, Chattopadhyay PK. Evolutionary programming techniques for economic load dispatch. IEEE Trans Evol Comput 2003;3(7):83–94.
[58] Park JB, Lee KS, Shin JR, Lee KY. A particle swarm optimization for economic dispatch with non-smooth cost functions. IEEE Trans Power Syst 2005;20(1):34–42.
[59] Arul R, Ravi G, Velusami S. Non-convex economic dispatch with heuristic load patterns, valve point effect, prohibited operating zones, ramp-rate limits and spinning reserve constraints using harmonic search algorithm. Electr Eng 2013;95:53–61.
[60] Bhattacharya A, Roy PK. Solution of multi-objective optimal power flow using gravitational search algorithm. IET Gener Transm Distrib 2012;6(8):751–63.
[61] Bhattacharya A, Chattopadhyay PK. Application of biogeography-based optimization to solve different optimal power flow problems. IET Gener Transm Distrib 2011;5(1):70–80.
[62] Duman Serhat, Guvenc Ugur, Sonmez Yusuf, Yorukeren Nuran. Optimal power flow using gravitational search algorithm. Energy Convers Manage 2012;59:86–95.
[63] http://shodhganga.inflibnet.ac.in/bitstream/10603/1221/18/18_appendix.pdf.

**Ch. V. Suresh** is currently pursuing Ph.D. in the Department of Electrical and Electronics Engineering, University College of Engineering Kakinada, Jawaharlal Nehru Technological University Kakinada, Kakinada, AP, India. His interests include, Computer Applications in Power Systems, Optimization Techniques, FACTS, Power System Analysis including FACTS devices and Power System Operation and Control.

**S. Sivanagaraju** is Professor in the Department of Electrical and Electronics Engineering, University College of Engineering Kakinada, Jawaharlal Nehru Technological University Kakinada, Kakinada, AP, India. He completed his Master degree from Indian Institute of Technology, Khargpur, India, in electrical power systems. He completed his doctoral program from Jawaharlal Nehru Technological University Hyderabad, Andhra Pradesh, India. His interests include FACTS Controllers, Electrical Distribution System Automation, Optimization Techniques, Voltage Stability, Power System Analysis, and Power System Operation and Control.